

Analytical Expression for Low-dimensional Resonance Island in 4-dimensional Symplectic Map

Shin-itiro GOTO

*Department of Applied Mathematics and Physics, Kyoto University, Kyoto
606-8501, Japan*

We study a 2- and a 4-dimensional nearly integrable symplectic maps using a singular perturbation method. Resonance island structures in the 2- and 4- dimensional maps are successfully obtained. Those perturbative results are numerically confirmed.

§1. Introduction

Chaotic Hamiltonian systems with many degrees of freedom are not only of interest in view of the foundation of dynamical system, but also have a lot of applications. Classical Hamiltonian mechanics has been applied to various physical problems, such as chemical reactions, plasma physics and solar systems.¹⁾ Although it is important to study such systems, we cannot understand the global flow generated by a Hamiltonian in the phase space due to the high-dimensionality. For a low-dimensional system, the phase space is visualized and then one overinterprets high-dimensional Hamiltonian flows beyond ones in a 2-dimensional phase space, but such imaginations are not guaranteed.

On the other hand, the origin of the global Hamiltonian chaos is an overlap of two resonance islands in the phase space.¹⁾ Then a fundamental problem for the study of Hamiltonian chaos is to analyze a resonance structure. To tackle this problem for systems with many degrees of freedom, we take a singular perturbation method. Using a systematic singular perturbation method, we can show the functional form of an island structure even for high-dimensional systems without information on the geometry of the phase space.

In this article, we take a renormalization method which is one of singular perturbation methods. All sorts of renormalization methods remove secular or divergent terms from a naive perturbation series by renormalized integration constants of the non-perturbation solution, and each prescription of the method does not depend on the detail of a given system.^{2)–5)} One of the reformulated renormalization method which we take here is easily applied to non-chaotic systems and also chaotic maps.^{5)–7)} Using this reformulated renormalization method, we tackle the standard map defined in 2-dimensional phase and the Froeschlé map defined in 4-dimensional phase space. Both maps are chaotic and are known for the standard models to study Hamiltonian chaos.

§2. The Standard map

To begin with, we study a resonance structure in the standard map¹⁾ $(x^n, y^n) \mapsto (x^{n+1}, y^{n+1})$

$$\begin{aligned} x^{n+1} &= x^n + y^{n+1}, \quad (\text{mod } 2\pi) \\ y^{n+1} &= y^n + \varepsilon \sin(x^n). \quad (\text{mod } 2\pi) \end{aligned}$$

Here x^n and y^n are the canonical variables, $n \in \mathbb{Z}$ denotes the discrete time and $\varepsilon (0 < \varepsilon \ll 1)$ is the small parameter, and this map is symplectic ($dx^{n+1} \wedge dy^{n+1} = dx^n \wedge dy^n$). Eliminating y variable, we have

$$Lx^n = \varepsilon \sin(x^n), \quad (\text{mod } 2\pi) \quad (2.1)$$

where $Lx^n := x^{n+1} - 2x^n + x^{n-1}$. A naive perturbation solution shows where a resonance island appears, and the structure can be obtained using our renormalization method. In our case, the naive perturbation series expansion $x^n = x^{(0)n} + \varepsilon x^{(1)n} + \varepsilon^2 x^{(2)n} + \mathcal{O}(\varepsilon^3)$ is obtained by solving $Lx^{(0)n} = 0$, $Lx^{(1)n} = \sin(x^{(0)n})$, $Lx^{(2)n} = x^{(1)n} \cos(x^{(0)n}), \dots$, where $(\text{mod } 2\pi)$ operation is taken into account in each equation. The non-perturbative solution is given by $x^{(0)n} = a + nP$, where a and P are the integration constants. Here P is the value of $y^{(0)n}$, due to the relation $y^{(0)n+1} := x^{(0)n+1} - x^{(0)n} = P$. Then the values of P and a are in $[0, 1)$. The naive perturbation solution up to $\mathcal{O}(\varepsilon^2)$ is classified by the value of P as follows

$$\begin{aligned} x^n &= a + nP + \varepsilon \frac{-\sin(a + nP)}{4 \sin^2(P/2)} + \varepsilon^2 \frac{\sin(2(a + nP))}{32 \sin^2(P) \sin^2(P/2)} \\ &\quad + \mathcal{O}(\varepsilon^3), (\text{mod } 2\pi), \quad (P \neq 0, \pi) \\ x^n &= a + \varepsilon \frac{\sin(a)}{2} n^2 + \varepsilon^2 \frac{\sin(2a)}{48} (n^4 - n^2) + \mathcal{O}(\varepsilon^3), (\text{mod } 2\pi) \quad (P = 0) \\ x^n &= a + \pi n + \varepsilon \frac{-\sin(a + \pi n)}{4} + \varepsilon^2 \frac{-\sin(2a)}{16} n^2 \\ &\quad + \mathcal{O}(\varepsilon^3), (\text{mod } 2\pi) \quad (P = \pi) \end{aligned} \quad (2.2)$$

Here we concentrate on the case of $P = \pi$ as an example. In the series (2.2), the secular behavior ($\propto \varepsilon^2 n^2$) appears. The renormalization method removes the secular terms in a systematic way. First we define the renormalized variable a^n as follows,

$$a^n := a + \varepsilon^2 \frac{-\sin(2a)}{16} n^2. \quad (2.3)$$

This definition (2.3) should include all secular term up to $\mathcal{O}(\varepsilon^2)$ in (2.2) and the integration constant, a , coming from the non-perturbative problem. The way to define a renormalized variable is quite similar to one in the case of a differential equation.⁵⁾ The renormalization equation is the map satisfying a^n perturbatively, and we impose here that the renormalization map which we would like to obtain is symplectic and autonomous. This is because the original map (2.1) has these two

properties. From the definition of the renormalized variable (2.3), we have

$$La^n = L\left(a + \varepsilon^2 \frac{\sin(2a)}{16} n^2\right) = -\varepsilon^2 \frac{\sin(2a)}{8}.$$

To obtain the map containing a^n only, we substitute $a = a^n + \mathcal{O}(\varepsilon)$ coming from the definition (2.3) into the relation $La^n = -\varepsilon^2 \sin(2a)/8$. Then we have the following renormalization map,

$$La^n = -\varepsilon^2 \frac{\sin(2a^n)}{8}. \quad (2.4)$$

When we introduce the new variable b^n defined as $b^{n+1} := a^{n+1} - a^n$, it turns out that this renormalization map (2.4) is automatically symplectic ($da^{n+1} \wedge db^{n+1} = da^n \wedge db^n$). It is noted here that the reduced map (2.4) is also obtained using another singular perturbation method, and the similarity of the two maps (2.1) and (2.4) gives a self-similarity in the phase space.⁸⁾

From Eqs. (2.2) and (2.3), the relations between the renormalized variable a^n and the original variables (x^n, y^n) are obtained as

$$\begin{aligned} x^n &= a^n + \pi n - \frac{\varepsilon}{4} \sin(a^n + \pi n) + \mathcal{O}(\varepsilon^3), \pmod{2\pi} \\ y^n &= (a^n - a^{n-1}) + \pi - \frac{\varepsilon}{2} \sin(a^n + \pi n) + \mathcal{O}(\varepsilon^3). \pmod{2\pi} \end{aligned}$$

The unstable manifold of the renormalization map reproduces the resonance island located near $y = \pi$ in the original system (2.1). Fig. 1 shows that the phase space reconstructed using our renormalization method is close to one obtained by the original map even with $\varepsilon = 0.98$. Intuitively, this perturbative analysis is valid only for the case $0 < \varepsilon \ll 1$, however, Fig.1 shows that the validity of our renormalization map seems to be wider than $0 < \varepsilon \ll 1$ practically. To determine the actual validity of this analysis, we need a rigorous mathematical estimate. At any rate, it turns out that our renormalization method is also useful even for chaotic maps, and that our analysis could not be restricted in 2-dimensional maps.

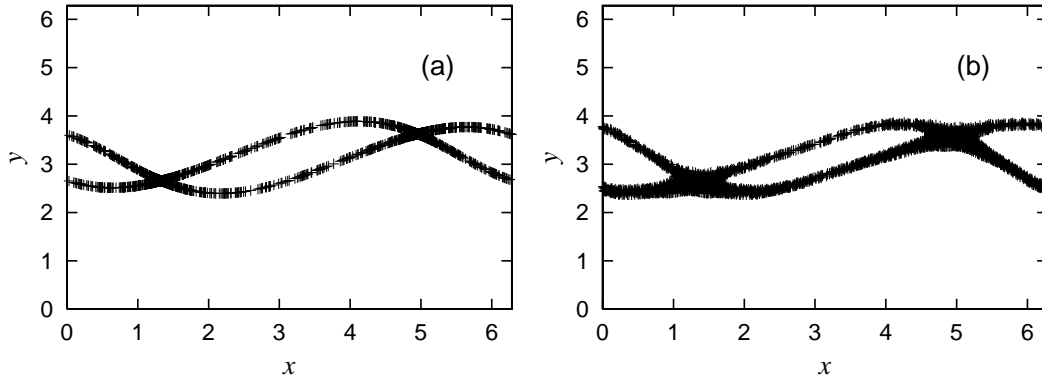


Fig. 1. The resonance island near $y = \pi$. For both figures the value of ε is 0.98, and the number of the initial condition is 1. (a): using the renormalization method, (b): obtained by the original map (2.1).

§3. The Froeschlé map

Next, we would like to study a 4-dimensional symplectic map. It is expected that a similar analysis gives a functional form of a resonant island even in a high-dimensional map, and it will be confirmed later in this section. The map which we study here is the Froeschlé map,⁹⁾ $(x_1^n, x_2^n, y_1^n, y_2^n) \mapsto (x_1^{n+1}, x_2^{n+1}, y_1^{n+1}, y_2^{n+1})$, $(\sum_{j=1}^2 dx_j^{n+1} \wedge dy_j^{n+1} = \sum_{j=1}^2 dx_j^n \wedge dy_j^n)$

$$\begin{aligned} y_1^{n+1} &= y_1^n + \frac{\varepsilon A_1}{2\pi} \sin(2\pi x_1^n) + \frac{\varepsilon C}{2\pi} \sin(2\pi(x_1^n + x_2^n)), \quad (\text{mod } 1) \\ y_2^{n+1} &= y_2^n + \frac{\varepsilon A_2}{2\pi} \sin(2\pi x_2^n) + \frac{\varepsilon C}{2\pi} \sin(2\pi(x_1^n + x_2^n)), \quad (\text{mod } 1) \\ x_1^{n+1} &= x_1^n + y_1^{n+1}, \quad (\text{mod } 1) \\ x_2^{n+1} &= x_2^n + y_2^{n+1}. \quad (\text{mod } 1) \end{aligned}$$

Here $n \in \mathbb{Z}$ denotes the discrete time, x_1^n, x_2^n and y_1^n, y_2^n are the canonical variables, A_1, A_2, C are the parameters and $\varepsilon (0 < |\varepsilon| \ll 1)$ is the perturbation parameter. The Froeschlé map⁹⁾ has numerically been studied for the Arnold diffusion¹⁾ as one of canonical 4-dimensional maps in several papers.¹⁰⁾ Eliminating y_1^n and y_2^n variables, we have

$$Lx_j^n = \frac{\varepsilon A_j}{2\pi} \sin(2\pi x_j^n) + \frac{\varepsilon C}{2\pi} \sin(2\pi(x_1^n + x_2^n)), \quad (\text{mod } 1), \quad (j = 1, 2)$$

where $Lx_j^n := x_j^{n+1} - 2x_j^n + x_j^{n-1}$, $(j = 1, 2)$. The naive perturbation solutions $x_j^n = x_j^{(0)n} + \varepsilon x_j^{(1)n} + \mathcal{O}(\varepsilon^2)$, $(j = 1, 2)$ are obtained by solving the following equations,

$$\begin{aligned} Lx_j^{(0)n} &= 0, \quad (\text{mod } 1) \quad (j = 1, 2) \\ Lx_j^{(1)n} &= \frac{A_j}{2\pi} \sin(2\pi x_j^{(0)n}) + \frac{C}{2\pi} \sin(2\pi(x_1^{(0)n} + x_2^{(0)n})). \quad (\text{mod } 1) \quad (j = 1, 2) \end{aligned}$$

The non-perturbative solutions are $x_j^{(0)} = a_j + nP_j$, $(j = 1, 2)$. Here a_j and P_j are the integration constants, and the values of them are in $[0, 1)$. The naive perturbation solutions are classified by the values of P_1 and P_2 , the solutions up to $\mathcal{O}(\varepsilon)$ are

$$\begin{aligned} x_j^n &= a_j + nP_j + \varepsilon \left(\frac{A_j}{4\pi} \frac{\sin(2\pi(a_j + nP_j))}{\cos(2\pi P_j) - 1} + \frac{C}{4\pi} \frac{\sin(2\pi(a_1 + nP_1) + 2\pi(a_2 + nP_2))}{\cos(2\pi(P_1 + P_2)) - 1} \right) \\ &\quad + \mathcal{O}(\varepsilon^2), \quad (\text{mod } 1), \quad (P_1 \neq 0, P_2 \neq 0, P_1 + P_2 \neq 0) \end{aligned} \quad (3.1)$$

$$\begin{aligned} x_j^n &= a_j + nP_j + \varepsilon \left(\frac{A_j}{4\pi} \frac{\sin(2\pi(a_j + nP_j))}{\cos(2\pi P_j) - 1} + \frac{C}{4\pi} n^2 \sin(2\pi(a_1 + a_2)) \right) \\ &\quad + \mathcal{O}(\varepsilon^2), \quad (\text{mod } 1) \quad (P_1 \neq 0, P_2 \neq 0, P_1 + P_2 = 0) \end{aligned} \quad (3.2)$$

$$\begin{aligned} x_j^n &= a_j + \varepsilon \left(\frac{A_j}{4\pi} n^2 \sin(2\pi a_j) + \frac{C}{4\pi} n^2 \sin(2\pi(a_1 + a_2)) \right) \\ &\quad + \mathcal{O}(\varepsilon^2), \quad (\text{mod } 1) \quad (P_1 = 0, P_2 = 0) \end{aligned} \quad (3.3)$$

and the solutions at $P_1 = 0, P_2 \neq 0$ are calculated as

$$x_1^n = a_1 + \varepsilon \left(\frac{A_1}{4\pi} n^2 \sin(2\pi a_1) + \frac{C}{4\pi} \frac{\sin(2\pi a_1 + 2\pi(a_2 + nP_2))}{\cos(2\pi P_2) - 1} \right) + \mathcal{O}(\varepsilon^2), (\text{mod}1) \quad (3.4)$$

$$x_2^n = a_2 + nP_2 + \varepsilon \left(\frac{A_2}{4\pi} \frac{\sin(2\pi(a_2 + nP_2))}{\cos(2\pi P_2) - 1} + \frac{C}{4\pi} \frac{\sin(2\pi a_1 + 2\pi(a_2 + nP_2))}{\cos(2\pi P_2) - 1} \right) + \mathcal{O}(\varepsilon^2), (\text{mod}1). \quad (3.5)$$

The solutions at $P_1 \neq 0, P_2 = 0$ are obtained by exchanging the suffixes 1 and 2 in Eqs. (3.4) and (3.5). We consider the case that the low-dimensional resonance island appears located at $P_1 = 0, P_2 \neq 0$ so that we can easily check the validity of our analysis numerically. If one considers the case (3.1), then there is no resonance island up to this approximation. Furthermore one considers the cases (3.2) and (3.3), there are resonance islands described by 4-dimensional maps. For the case of $P_1 = 0, P_2 \neq 0$, a secular term ($\propto \varepsilon n^2$) appears in Eq.(3.4), however, does not appear in Eq. (3.5). To remove the secular term in Eq.(3.4), we define the renormalized variable

$$a_1^n := a_1 + \varepsilon \frac{A_1}{4\pi} n^2 \sin(2\pi a_1). \quad (3.6)$$

From the definition (3.6), we obtain the symplectic renormalization map

$$La_1^n = \varepsilon \frac{A_1}{2\pi} \sin(2\pi a_1^n). \quad (3.7)$$

This procedure to obtain the renormalization map (3.7) is the same as the case for the standard map in §2. The renormalization map (3.7) is symplectic and has the form of the standard map. Since the renormalization map of the standard map is the standard map itself (see Eqs.(2.1) and (2.4)), a self-similar structure of the phase space could be obtained when one considers the renormalization map (3.7).

From Eqs.(3.4)-(3.5) and Eq. (3.6), we have the following relation between the renormalized variable a_1^n and the original variables (x_1^n, x_2^n)

$$x_1^n = a_1^n + \varepsilon \frac{C}{4\pi} \frac{\sin(2\pi a_1^n + 2\pi(a_2 + nP_2))}{\cos(2\pi P_2) - 1} + \mathcal{O}(\varepsilon^2), (\text{mod}1) \quad (3.8)$$

$$x_2^n = a_2 + nP_2 + \varepsilon \left(\frac{A_2}{4\pi} \frac{\sin(2\pi(a_2 + nP_2))}{\cos(2\pi P_2) - 1} + \frac{C}{4\pi} \frac{\sin(2\pi a_1^n + 2\pi(a_2 + nP_2))}{\cos(2\pi P_2) - 1} \right) + \mathcal{O}(\varepsilon^2), (\text{mod}1) \quad (3.9)$$

and the other original variables y_1^n and y_2^n are obtained as $y_1^n = x_1^n - x_1^{n-1}$ and $y_2^n = x_2^n - x_2^{n-1}$. The unstable manifold of the renormalization map (3.7) and Eqs. (3.8)–(3.9) reproduce the low-dimensional resonance island in the ambient phase space of the system. Figs. 2 and 3 show that our analysis can predict the low-dimensional resonance island even in 4-dimensional phase space. Due to this success of the prediction, we understand that the low-dimensional resonance island

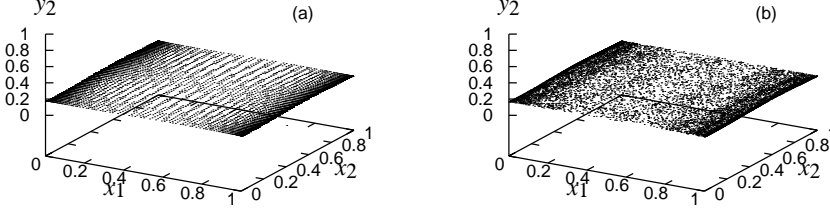


Fig. 2. The phase portrait near the resonance island characterized by $P_1 = 0, P_2 \neq 0$, parameters are $P_2 = 0.18(\neq 0), \varepsilon A_1 = 0.04, \varepsilon A_2 = 0.05, \varepsilon C = 0.02$. The number of the initial condition is 1. (a): obtained by the renormalization method, and (b): calculated using the original map.

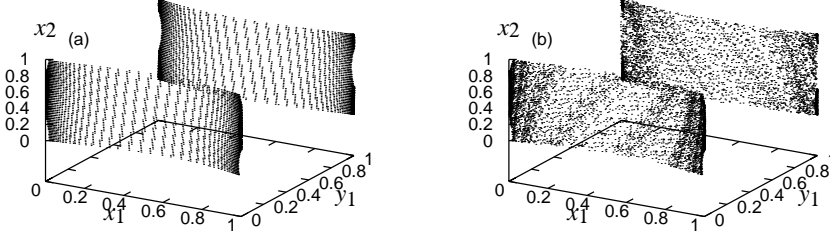


Fig. 3. The phase portrait near the resonance island characterized by $P_1 = 0, P_2 \neq 0$. The parameters are given in the caption to Fig. 2. (a): obtained by the renormalization method, and (b): calculated using the original map.

has the same functional form as in the 2-dimensional standard map. To confirm the description of the approximate low-dimensional resonant island further, we plot a projection of the manifold onto the space spanned by x_1 and y_1 as shown in Fig. 4, and it certainly suggests the success of the analysis with the perturbation strength $0 < |\varepsilon| \lesssim 0.01$. Although we do not show any figure, our perturbative analysis fails when ε is bigger than $\varepsilon_* \sim 0.01$ for $P_1 = 0$ and $P_2 = 0.18$. Taking into account Fig. 1, one finds that the regime $0 < |\varepsilon| \lesssim \varepsilon_*$ in which we can use a perturbation analysis for the Froeschlé map is narrower than that for the standard map in §2. A mathematical estimate is needed to determine the actual validity of our analysis again, as stated in §2. On the other hand, according to the expressions for the naive perturbation solutions (3.3)–(3.5), it is natural to expect that the renormalization map (3.7) fails when P_2 approaches to 0, and we have numerically confirmed that ε_* generally depends on P_2 for $P_1 = 0$. A situation where the integration constant P_2 narrows the regime $0 < |\varepsilon| \lesssim \varepsilon_*$ does not appear in 2-dimensional maps, and is one of features in high-dimensional maps.

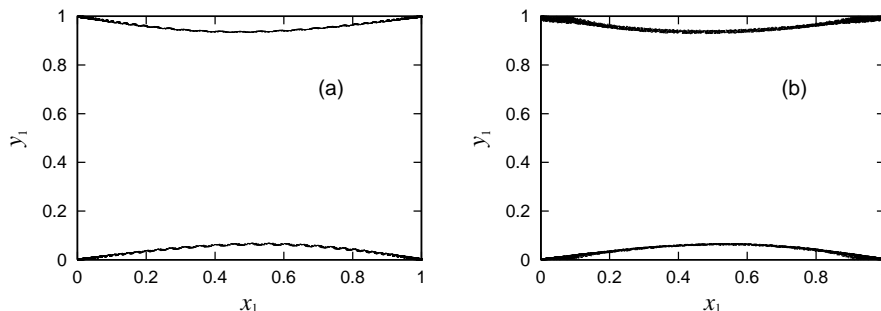


Fig. 4. The phase portrait near the resonance island characterized by $P_1 = 0, P_2 \neq 0$. The parameters are given in the caption to Fig. 2. (a): obtained by the renormalization method, and (b): calculated using the original map.

§4. Conclusions

In this article, we have analyzed a 2- and a 4-dimensional symplectic maps using a renormalization method. For both maps, we have successfully reduced their resonance island analytically and the perturbative reductions have been confirmed numerically. Although a resonance island is the most fundamental object to study global Hamiltonian chaos for a system with any degrees of freedom, the island structure cannot be visualized for a system with many degrees of freedom. This study shows how a low-dimensional island appears in the Froeschlé map, at least in a nearly integrable regime. The method which we have used here is also useful for a wider class of symplectic maps, and then this analysis shed light on the study of the Hamiltonian systems with many degrees of freedom.

Acknowledgments

The author thanks the members of the laboratory of dynamical systems theory, Kyoto University, for their comments and encouragements. The author has been supported by a JSPS Fellowship for Young Scientists.

References

- 1) A.J. Lichtenberg and M.A. Lieberman, *Regular and Chaotic Dynamics* (Springer, Berlin, 1992).
- 2) L.Y. Chen, N. Goldenfeld and Y. Oono, Phys. Rev. Lett. **73** (1994), 1311 ; L.Y. Chen, N. Goldenfeld and Y. Oono, Phys. Rev. E. **54** (1996), 376 .
- 3) Y. Oono, Int. J. Mod. Phys. B. **14** (2000), 1327 .
- 4) T. Kunihiro, Prog. Theor. Phys. **94** (1995), 503 ; T. Kunihiro, Prog. Theor. Phys. **97** (1997), 179 ; T. Kunihiro and J. Matsukidaira, Phys. Rev. E **57** (1998), 4817.
- 5) S. Goto, Y. Masutomi and K. Nozaki, Prog. Theor. Phys. **102** (1999), 471.
- 6) Y. Masutomi and K. Nozaki, Physica D. **151** (2001) 44; S. Kawaguchi, Prog. Theor. Phys. **113** (2005) 687.
- 7) S. Goto and K. Nozaki, Prog. Theor. Phys. **105** (2001), 99; S. Goto and K. Nozaki, J. Phys. Soc. Jpn. **70** (2001), 49; S. Goto, K. Nozaki and H. Yamada, Prog. Theor. Phys. **107** (2002), 637; S.I. Tzenov and R.C. Davidson, New Journal of Physics, **5** (2003), 67; S. Goto and K. Nozaki, Physica D. **194** (2004), 175; T. Maruo, S. Goto and K. Nozaki,

- Prog. Theor. Phys. **111** (2004), 463.
- 8) D.S. Broomhead and G. Rowlands, J. Phys. A. **16** (1983), 9.
 - 9) C. Froeschlé, Astrophys. SpaceSci. **14** (1971), 110.
 - 10) For exmaple, B.P. Wood, A.J. Lichtenberg and M.A. Lieberman, Phys. Rev. A 42 (1990) 5885; S. Honjo and K. Kaneko, Advances in Chemical Physics 130 part B (2005)437.